On the Impact of Microgrid Energy Management Systems on Power System Dynamics

P. Ferraro,† *Student Member, IEEE*, E. Crisostomi,† *Senior Member, IEEE*, M. Raugi,† and F. Milano,‡ *Fellow, IEEE*
† Department of Energy, Systems, Territory and Constructions Engineering, University of Pisa, Italy
‡ School of Electrical and Electronic Engineering, University College Dublin, Belfield, Ireland

***Abstract*— This paper compares the impact of microgrids on the transient response of the transmission system, and, more specifically, on its frequency variations, when different control strategies and different storage capacities are employed. Extensive Monte Carlo simulations are performed based on the IEEE 39-bus system, and show that the dynamic behavior of the transmission system is affected in a non-trivial way by the control strategy of the microgrids energy management system and their storage capacity.**

I. Introduction

A. Motivation

The continuous increase of the energy generated from renewable sources, capillary distributed in vast areas, is changing the traditional top-down shape of power grids into a network of flexible smart small-sized power systems, denoted as Microgrids (MGs). While it may be hard to give a precise definition of a MG, a practical one provided by the U.S. Department of Energy is that *a MG is a group of interconnected loads and DERs with clearly defined electrical boundaries that acts as a single controllable entity with respect to the grid and can connect and disconnect from the grid to enable it to operate in both grid-connected or island mode* [1]. Consistently to this definition, MGs are expected to become the building blocks of the future power grid [2]. An interesting aspect that has not been fully explored in the literature related to MGs, is how the interactions among MGs may impact on the dynamics of the overall grid, and this aspect is here investigated in the paper.

B. Literature Review

Several recent works focus on the control of *individual*, often islanded, MGs and on the impact of Distributed Energy Resources (DERs) on grid dynamics, for instance in terms of frequency and voltage stability of the grid. A review on the impact of low rotational inertia in the power system has been presented in [3]. In [4], angle and voltage stability are analyzed as the MG penetration level increases and, in [5] and [6], the effects of the penetration of wind- and PV solar-based DERs, respectively, are investigated. These works, however, do not consider the ability of a MG to conduct policies of Demand Response (DR), its interaction with the market, and its impact on the transient response of the transmission system.

On the other hand, it is the authors' opinion that, to fully understand MG operation and dynamics, it is not sufficient to consider an individual MG and ignore the interactions among MGs, the grid and the electrical market. A first step in this direction was given in [7], where the authors showed that it is more convenient when coordinated MGs cooperate to solve the power scheduling problem; however, dynamic and stability issues of the grid were not deeply investigated in [7]. In our work [8], we investigated the interactions between MGs, the electrical market and the transmission system when MGs sell and buy energy from the grid according to their economical convenience. The main result of [8] is that a configuration with few large or several small coordinated MGs can drastically deteriorate the transient behavior of the grid and reduce its stability margins. On the other hand, a high-granularity and non-coordinated configuration with several small MGs appears to be more convenient for a proper operation of the system.

This paper further elaborates on the model described in [8] and evaluates what happens if MGs do not compete in the electricity market but rather minimize the power exchange with the grid. In particular, we assume that the MGs operate in island mode as long as possible, i.e., utilizing the storage reserve whenever possible, and buying and selling energy only when strictly necessary. Accordingly, we compare the outcomes of this new framework with the ones of [8]. In this paper, we also evaluate the impact of different storage sizes in the MGs.

C. Contributions

The objective of this paper is to quantitatively evaluate the impact of MGs on the stability of the grid. While there is a general consensus that the uncertainty in a grid, and thus, its complexity, grows with respect to the number of installed renewable generations, in this paper, we show that other factors may affect the stability of the grid; namely, the energy policies of the MGs (i.e., whether they collaborate or compete in the energy market), and the size of their storage devices (as these affect the ability of the MGs to operate in island mode).

The impact of MG control and Energy Management System (EMS) is evaluated though computing the frequency deviations of the grid. Frequency deviations are a measure of the active power imbalance and should remain within the operational limits in order to avoid transmission line overloads and the triggering of protection devices [9]. Since MGs are expected to buy and sell active power according to their DR policies, the magnitude of frequency deviations is an important metric to assess the impact of the penetration of MGs on the grid. The standard deviation of the frequency of the Center Of Inertia (COI) of the system is the specific metric that we utilize to evaluate the impact of MGs on the grid dynamic response.

D. Organization

The remainder of the paper is organized as follows. Section II describes the modeling of the power system, of the electricity market, as well as of MGs and their control strategies. Section III presents a case study based on the IEEE 39-bus system. In the case study, the dynamic impact on the grid of the MGs is thoroughly evaluated through a Monte Carlo method and stochastic time domain simulations. Main conclusions and future work are outlined in Section IV.

II. Modeling

For the purposes of this paper, the MG is modeled as a cluster of loads and generation units, coordinated by an EMS that, among other tasks (e.g., load shedding and internal power flow management), allows the MG to operate in island mode (i.e., the MG operates autonomously from the power grid) and determines the set point of the active power that the MG sells or buys from the electrical grid [10].

The following assumptions are made:

- The internal dynamics of the control system, generation units and loads of a MG are neglected. This assumption is based on the observation that the time constants of the internal MG dynamics are small compared to the ones of the high voltage transmission system [11]–[13].
- The storage units, the DERs and the loads of each MG are grouped into an aggregated model. This assumption can be relaxed, assuming distributed DERs, storage units and loads at the expense of a higher computational burden.

The metric utilized to compare the effects of different EMSs and storage capacity sizes is the COI frequency, defined as

$$\omega_{COI} = \frac{\sum_{i=1}^{r} H_i \omega_i}{\sum_{i=1}^{r} H_i}, \tag{1}$$

where ω_i and H_i are, respectively, the rotor speed and the inertia constant of the i-th synchronous machine, and r is the number of conventional generators in the grid.

A. Power System Model

The model of the power system considered in the case study is based on the conventional set of hybrid differential algebraic equations [14], as follows:

$$\begin{aligned} \dot{\boldsymbol{x}} &= \boldsymbol{f}(\boldsymbol{x}, \boldsymbol{y}, \boldsymbol{u}) \\ \boldsymbol{0} &= \boldsymbol{g}(\boldsymbol{x}, \boldsymbol{y}, \boldsymbol{u}) \end{aligned} \tag{2}$$

where $\boldsymbol{f}$ ($\boldsymbol{f} : \mathbb{R}^{p+q+s} \mapsto \mathbb{R}^p$) are the differential equations; $\boldsymbol{g}$ ($\boldsymbol{g} : \mathbb{R}^{p+q+s} \mapsto \mathbb{R}^q$) are the algebraic equations; $\boldsymbol{x}$ ($\boldsymbol{x} \in \mathbb{R}^p$) are the state variables; $\boldsymbol{y}$ ($\boldsymbol{y} \in \mathbb{R}^q$) are the algebraic variables; and $\boldsymbol{u}$ ($\boldsymbol{u} \in \mathbb{R}^s$) are discrete events, which mostly model MG EMS logic.

Equations in (2) include conventional dynamic models of synchronous machines (e.g., 6th order models), their controllers, such as, automatic voltage regulators, turbine governors, and power system stabilizers, as well as lumped models of the transmission system, market dynamics, and the MG components, such as DERs, storage devices and loads. More details on the MG devices are provided in Subsection II-C.

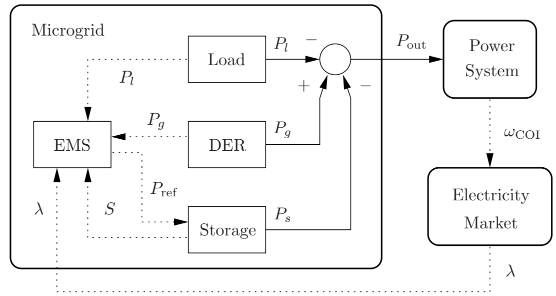

Fig. 1: Structure of the connection between the MG.

B. Electricity Market Model

In this work, we are interested in investigating the impact on the grid of a number of MGs that try to work in island mode as much as possible. In such a framework, the market model does not play a relevant role. However, since we compare results with those obtained in [8], where the MGs were assumed to operate with the objective of maximizing their revenues, it is relevant to briefly outline the dynamic electricity market model utilized in [8]. Such a model in based on [15], where power system dynamics are assumed to be coupled with a real-time – or *spot* – electricity market, also modeled based on differential equations. These represent an ideal market for which the energy price λ, assumed to be a continuous state variable, is computed and adjusted rapidly enough with respect to the dynamic response of the transmission system, e.g., PJM, California, etc. Further details can be found in [15] and [8].

C. Microgrid Model

Figure 1 shows the connections of the MG with the power system and the electricity market. The elements that compose the MG are the load, the DER, the storage device and the energy management system (EMS) that decides the operation mode of the MG and imposes its power generation set point.

The dynamic of the aggregated storage device model is ruled by the following equation, which is the continuous-time equivalent of the model used in [16],

$$T_c \dot{S} \;=\; P_s \;=\; P_g - P_l - P_{\text{out}} \tag{3}$$

where S is the state of charge of the MG, T_c is the time constant of the storage active power controller, P_s is the power generated or absorbed by the storage device ($P_s > 0$ if the storage is charging); P_{out} is the power output of the MG; and P_g and P_l are the produced active power and the local loads, respectively, of the MG. S undergoes an anti-wind-up limiter that models the charged ($S = 1$) and discharged ($S = 0$) conditions.

The dynamic model of the DER that is included in the MG is based on the DER models discussed in [17], [18]. The control scheme included in the DER model is shown in Fig. 2.

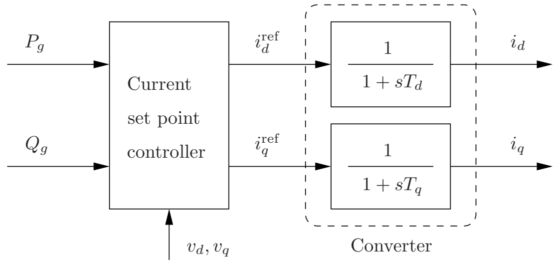

Fig. 2: Control scheme of an converter-based DER.

The power injections into the ac bus are:

$$\begin{aligned} P_g &= v_d i_d + v_q i_q \\ Q_g &= v_q i_d - v_d i_q \end{aligned} \tag{4}$$

where i_d and i_q are the ac-side dq-frame currents of the VSC, respectively and v_d and v_q are the dq-frame components of the bus voltage phasor of the point of connection of the VSC with the ac grid.

Uncertainty and volatility of both generation units and loads are accounted for by modeling the net power produced by the MG as a stochastic process according to

$$P_{\mathrm{net}} \;=\; P_g - P_l \;=\; \bar{P}_{g_T} - \bar{P}_{l_T} + \eta_M \tag{5}$$

where η_M is a white noise as in [19] with standard deviation σ_M, and $\bar{P}_{g_T}$ and $\bar{P}_{l_T}$ are piece-wise constant functions that account for uncertainty and change randomly with a period T as discussed in [20]. The noise is modeled as a single stochastic state variable as the behavior of the MG depends on the difference $P_{\mathrm{net}} = P_g - P_l$ and not on their absolute values. Finally, P_s, the power provided or absorbed by the aggregated storage device included in the MG is the slack variable that allows imposing the desired P_{ref}, as follows:

$$T_s \dot{P}_s \;=\; P_{\mathrm{out}} - P_{\mathrm{ref}} \;=\; -P_s + P_{\mathrm{net}} - P_{\mathrm{ref}}. \tag{6}$$

where T_s is the time constant of the storage active power controller and P_{ref} is the reference power set point as defined by the EMS of the MG.

D. Energy Management System of the Microgrid

In this paper, we evaluate a different strategy for the EMS that, as we shall see in the next section, has an opposite impact on the grid with respect to the EMS proposed on [8]. In particular, unlike [8], where the price λ plays a critical role, EMS input quantities are the produced power P_g, the load P_l and the state of charge of the storage units, S. The rules are divided into two sets: the seller state, for which $P_{\mathrm{net}} \geq 0$ (i.e., the MG is producing more than it is consuming and it will most likely sell energy) and the buyer state, for which $P_{\mathrm{net}} < 0$ (i.e., the MG is consuming more than it is producing and it will most likely buy energy). The objective of the EMS is to make the MG operate in island mode, if possible (i.e., $P_{\mathrm{ref}} = 0$). Thus, in seller mode each MG uses the active power surplus to charge its storage and sells it when fully charged, whereas in buyer mode, each MG discharges the storage when it has a high level of charge and buys the energy deficit when the state of charge is low.

TABLE I: Microgrid EMS rules

Seller mode, $P_{\mathrm{net}} \geq 0$		
Rule	**Action**	**Rationale**
if $S \leq 80\%$	$P_{\mathrm{ref}} = 0$	The battery is not fully charged, use the energy surplus to charge it
else	$P_{\mathrm{ref}} = P_{\mathrm{net}}$	Sell the surplus
Buyer mode, $P_{\mathrm{net}} < 0$		
Rule	**Action**	**Rationale**
if $S \geq 20\%$	$P_{\mathrm{ref}} = 0$	The battery has residual charge, use it to match the internal energy deficit
else	$P_{\mathrm{ref}} = P_{\mathrm{net}}$	Storage is low on charge, buy the energy deficit

The aforementioned rules are shown and explained in Table I. The rules are expressed hierarchically, i.e., a rule is evaluated only if the conditions of the previous ones are not satisfied.

III. Case Study

This section discusses the dynamic response of a system with inclusion of MGs regulated by means of the EMS described in the previous section. A comparison with the results obtained with the EMS model proposed in [8] is also presented. Two scenarios are considered, as follows.

a) *Small Storage Scenario.* An increasing number of large MGs, with small storage dimensions, is plugged into the system.
b) *Large Storage Scenario.* An increasing number of large MGs, with large storage dimensions, is plugged into the system.

Simulations are based on the IEEE 39-bus 10-machine system; this benchmark grid is chosen in order to have both a fairly complex network and reduced state-space dimensions to easily understand the impact of MGs on the system. The state-space of the simplest case with 1 MG includes 150 state variables and 233 algebraic ones; whereas the case with highest granularity includes 12 MGs, 204 state variables and 365 algebraic ones. The results for each scenario are obtained based on a Monte Carlo method (100 simulations are solved for each scenario).

Table II shows the parameters for the considered MGs, including the storage time constants in the two different scenarios. Note that we simulate different sizes of the storage by changing the charge/discharge time constant T_c in (3).

All simulations are performed using Dome, a Python-based power system software tool [21]. The Dome version utilized in this case study is based on Python 3.4.1; ATLAS 3.10.1 for dense vector and matrix operations; CVXOPT 1.1.8 for sparse matrix operations; and KLU 1.3.2 for sparse matrix factorization.

TABLE II: Parameters of MGs. The parameters $\sigma_{\rm net}$ are chosen in a random way for each MG to simulate different characteristics.

MG	Bus	$\bar{P}_g$ (pu MW)	$\bar{P}_l$ (pu MW)	$\sigma_{\rm net}$ (pu MW)	Small storage (s)	Large storage (s)
1	18	0.88	0.54	0.025	5.0	18,000.0
2	3	0.77	0.20	0.040	7.0	25,200.0
3	15	0.80	0.10	0.030	6.5	23,400.0
4	17	0.40	0.20	0.020	8.0	28,800.0
5	21	0.20	0.10	0.013	5.0	18,000.0
6	28	0.20	0.40	0.040	7.0	25,200.0
7	24	0.36	0.84	0.010	6.5	23,400.0
8	17	0.20	0.50	0.020	8.0	28,800.0
9	11	0.20	0.30	0.010	4.0	14,400.0
10	5	0.10	0.80	0.010	5.0	18,000.0
11	7	0.80	0.10	0.030	7.4	26,640.0
12	12	0.40	0.40	0.025	6.8	24,480.0

TABLE III: Standard deviation of the frequency COI as a function of the total installed capacity of MGs.

		Small storage ($\sigma_{\rm COI}$)		Large storage ($\sigma_{\rm COI}$)	
MGs #	Capacity (pu MW)	M-EMS (pu Hz)	I-EMS (pu Hz)	M-EMS (pu Hz)	I-EMS (pu Hz)
1	0.96	0.00246	0.00312	0.00498	0.00049
2	1.81	0.00319	0.00454	0.00532	0.00088
3	2.69	0.00322	0.00475	0.00641	0.00094
4	3.13	0.00391	0.00498	0.00701	0.00117
5	3.35	0.00442	0.00517	0.00741	0.00127
6	3.57	0.00498	0.00570	0.00775	0.00168
7	3.97	0.00517	0.00607	0.00796	0.00193
8	4.19	0.00554	0.00625	0.00848	0.00221
9	4.41	0.00581	0.00679	0.00863	0.00261
10	4.52	0.00597	0.00719	0.00926	0.00282
11	5.40	0.00623	0.00772	0.01089	0.00324
12	5.84	0.00689	0.00784	0.01259	0.00392

A. Simulation results

Figure 3 shows a realization of the frequency of the COI ($\omega_{\rm COI}$) of the 39-bus system with inclusion of 12 MGs considering small and large energy storage capacity scenarios and both Market-based EMS (M-EMS) and Island-based EMS (I-EMS). The following remarks are relevant:

M-EMS and I-EMS behave in a similar way when the storage devices are small: As one might expect, when the storage devices are too small, MGs can only buy (sell) energy when the generated energy is lower (greater) than the energy requested by the loads. This behaviour is independent from the specific EMS policy of the MG. This result can be noticed by comparing Figs. 3a and 3c.

Operation in island mode is more convenient than a competitive approach in terms of the grid frequency: When the storage devices are large enough, the MG have more flexibility to effectively operate in island mode (I-EMS), or alternatively to competitively participate to the market (M-EMS). By comparing Figs. 3b and 3d, it is evident that $\omega_{\rm COI}$ oscillations are greater when the MG operates according to an M-EMS policy. On the other hand, when the MGs operate in island mode, fluctuations are smaller (see Fig. 3d).

More detailed results can be found in Table III, that shows the standard deviation of the frequency of the COI ($\sigma_{\rm COI}$), vs. the number of MGs, the capacity of the storage devices and the EMS control strategy. In all cases, $\sigma_{\rm COI}$ increases monotonically as the number of MGs increases. Consistently with the results depicted in Fig. 3, and regardless of the number of MGs, $\sigma_{\rm COI}$ is always larger when smaller storage devices are available, regardless of the specific EMS.

Table III also shows that in the small storage scenario, the M-EMS causes smaller variations of $\omega_{\rm COI}$ than the I-EMS. This result is due to the fact that I-EMS-driven MGs, while attempting to operate in island mode, actually have to connect often to the grid to match power demand and generation. On the other hand, in the large capacity scenario, we have the opposite outcome. In this case, the large capacity of the storage allows the I-EMS-driven MGs to operate most of the time in island mode. The large values of $\sigma_{\rm COI}$ obtained for M-EMS-driven MGs indicate that MGs, operated with benefit-oriented control strategy, are a potential threat for the stability of the system.

As a concluding remark, it is worth saying that system operators' network codes fix standard frequency ranges as well as maximum frequency variations. For example, for the ENTSO-E system, the standard frequency range is ± 50 mHz and the maximum steady-state deviation is ± 200 mHz. These values are wider in case of small or islanded systems, e.g., in UK and Ireland, the standard frequency range is ± 200 mHz and the maximum steady-state deviation is ± 500 mHz. It is interesting to note that, depending on the EMS implementation, such ranges might not be satisfied. Hence, the dynamic appraisal presented in this paper can help validate the feasibility of a given EMS scheme.

IV. Conclusions

This work analyzes and compares the dynamic behavior of power systems with inclusion of MGs operated with two different EMS control strategies. An EMS aims at maximizing the benefit of the MGs, while the other one aims at operating the MGs islanded from the system. The effect of the size of the storage devices included in the MG is also discussed in the paper. The impact on the system is evaluated by means of the amplitude of the standard deviation of the frequency of the COI. The main result obtained from simulations is that the dynamic impact of MGs on the system is a combination of the size of the storage and the EMS rules. The minimum impact on the system is obtained for MGs that tend to operate in island mode and include large storage capacities. However, if the storage capacity is low, the impact due to MGs on the system is lower if the MG attempts to maximize their incomes. Thus, results suggest that the optimal size of the storage device, from the point of view of the outer grid stability, might depend on the control strategy of the MGs. Future works will focus on the dynamic impact on power system of MGs that provide ancillary services.

Acknowledgment

Federico Milano is funded by Science Foundation Ireland under Grant No. SFI/15/IA/3074; H2020-LCE-2016-2017 Project "RE-SERVE" under Grant No. 727481; and by

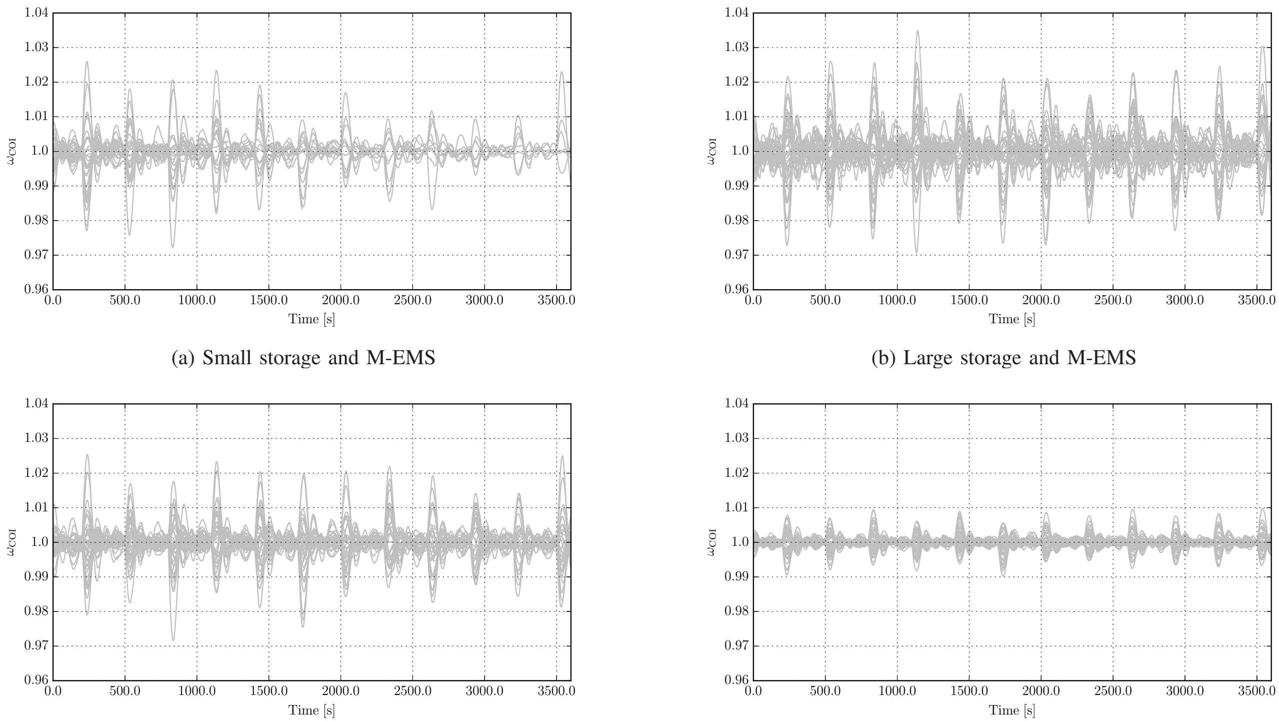

(a) Small storage and M-EMS

(b) Large storage and M-EMS

(c) Small storage and I-EMS

(d) Large storage and I-EMS

Fig. 3: Frequency of the COI of the 39-bus system with 12 MGs.

EC Marie Skłodowska-Curie Career Integration under Grant No. PCIG14-GA-2013-630811.

References

[1] S. Parhizi, H. Lotfi, A Khodaei and S. Bahramirad, *State of the Art in Research on Microgrids: A Review*, IEEE Access, Vol. 3, pp. 890-925, 2015.

[2] R. H. Lasseter and P. Piagi, *Microgrid: A Conceptual Solution*, Power Electronics Specialists Conference IEEE 35th Annual, Vol. 6, pp. 4285-4290, 2004.

[3] A. Ulbig, T. S. Borsche, and G. Andersson, *Impact of Low Rotational Inertia on Power System Stability and Operation*, IFAC, Vol. 47, pp. 72907297, 2014.

[4] J. Zhang, S. Su, J. Chen, and F. Hong, *Stability Analysis of the Power System with the Large Penetration Ratios of Microgrids*, SUPERGEN'09, pp. 1-5, 2009.

[5] L. Xie, P. M. S. Carvalho, L. A. F. M. Ferreira, J. Liu, B. H. Krogh, N. Popli, and M. D. Ilic, "Wind Integration in Power Systems: Operational Challenges and Possible Solutions," *Proceedings of the IEEE*, vol. 99, no. 1, pp. 214-232, Jan. 2011.

[6] J. T. Bialasiewicz, *Renewable Energy Systems With Photovoltaic Power Generators: Operation and Modeling*, IEEE Trans. on Industrial Electronics, vol. 55, no. 7, pp. 2752-2758, June 2008.

[7] A. Ouammi, H. Dagdougui, L. Dessaint, R. Sacile, *Coordinated Model Predictive-Based Power Flows Control in a Cooperative Network of Smart Microgrids*, IEEE Transactions on Smart Grid, Vol. 6, No. 5, pp. 2233-2243, 2015.

[8] P. Ferraro, E. Crisostomi, M. Raugi, F. Milano, *Stochastic Analysis of the Impact of Microgrid Penetration on Power System Dynamics*, accepted for publication, IEEE Transactions on Power Systems, 2017.

[9] H. Bevrani, *Robust Power System Frequency Control*, Springer, 2008.

[10] R. H. Lasseter, *Microgrid*, IEEE Power Engineering Society Winter Meeting, pp. 305-308, 2002.

[11] J. P. Guerrero, J. C. Vásquez, J. Matas, L. García de Vicuna, M. Castilla, *Hierarchical Control of Droop-Controlled AC and DC Microgrids – A General Approach Toward Standardization*, IEEE Trans. on Industrial Electronics, Vol. 58, No. 1, pp. 158-172, 2010.

[12] Q. Shafiee, J. C. Vásquez, and J. M. Guerrero. *A Distributed Secondary Control for Islanded MicroGrids. A Networked Control Systems Approach*, IECON 2012 - 38th Annual Conference on IEEE Industrial Electronics Society, pp. 5637-5642, 2012.

[13] N. Pogaku, M. Prodanović and T. C. Green., *Modeling, Analysis and Testing of Autonomous Operation of an Inverter-Based Microgrid*, IEEE Trans. on Power Electronics, Vol. 22, no. 2, pp. 613-625, March 2007.

[14] I. A. Hiskens, *Power System Modeling for Inverse Problems*, IEEE Trans. on Circuits and Systems I: Regular Papers, vol. 51, no. 3, pp. 539-551, March 2004.

[15] F. L. Alvarado, J. Meng , C. L. DeMarco and W. S. Mota, *Stability Analysis of Interconnected Power Systems Coupled with Market Dynamics*, IEEE Trans. on Power Systems, Vol. 16, no. 4, pp. 695-701, Aug. 2001.

[16] Wei-Yu Chiu, H. Sun, and H. V. Poor, *A Multiobjective Approach to Multimicrogrid System Design*, IEEE Trans. on Smart Grid, Vol. 6, No. 5, pp. 2263-2272, Aug. 2015.

[17] F. Milano, *Control and Stability of Future Transmission Networks*, in *The Handbook of Clean Energy Systems - Volume 4*, editor Prof. Jinyue Yan, John Wiley & Sons, June 2015.

[18] B. Tamimi, C. Cañizares and K. Bhattacharya, *Modeling and Performance Analysis of Large Solar Photo-Voltaic Generation on Voltage Stability and Inter-area Oscillations*, IEEE PES General Meeting, pp. 1-6, July 2011.

[19] F. Milano and R. Zárate-Miñano, *A Systematic Method to Model Power Systems as Stochastic Differential Algebraic Equations*, IEEE Trans. on Power Systems, vol. 28, no. 4, pp. 4537-4544, Nov. 2013.

[20] C. Roberts, E. M. Stewart, F. Milano, *Validation of the Ornstein-Uhlenbeck Process for Load Modeling Based on μPMU Measurements*, PSCC, pp. 1-7, June 2016.

[21] F. Milano, *A Python-based Software Tool for Power System Analysis*, IEEE PES General Meeting, pp. 1-5, July 2013.